

# Computing Medial Axis Transform with Feature Preservation via Restricted Power Diagram (Supplementary Material)

## ACM Reference Format:

. 2022. Computing Medial Axis Transform with Feature Preservation via Restricted Power Diagram (Supplementary Material). *ACM Trans. Graph.* 1, 1 (September 2022), 5 pages. <https://doi.org/10.1145/nnnnnnnn.nnnnnnnn>

## 1 MORE RESULTS

We ran our method on the first 100 models in the ABC dataset [Koch et al. 2019] under the *10k/test* folder using 2048 as the number of mesh vertices. There are 3/100 models with open boundaries, 9/100 models contains self-intersection and 25/100 models contains more than one connected components, summarized in Tab. 2. Since our method only focuses on closed, manifold triangulated model with no self-intersection and contains single connected component, we filter them down to 73/100 models that satisfy these requirements. Table 1 shows a summary statistics and the gallery is shown in Fig. 25 of the paper. For 26/73 models, we use Blender to remove degenerated faces (see Fig. 1 middle) for generating input with better quality. Those degenerated faces highly impact our detection of sharp features and also impact the calculation of RPD. All remeshed 26/73 models are marked in blue in Table. 1.

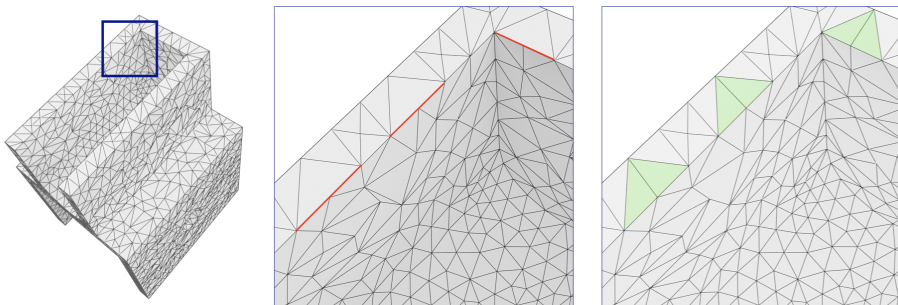


Fig. 1. Remesh the original model (left) by removing degenerated faces (middle, red) which results in a cleaner input mesh (right green) for our method.

As described in future work (Sec.7), even though we show experimental evidences that our computed MAT preserves topology for the majority of models we tested (54/73 in Tab. 1), our method does not guarantee the topological equivalence between the given shape and the medial mesh obtained from the dual of RPD. There are 19/73 models whose Euler characteristic deviates from ground truth. We will leave the topological investigation as our future work.

---

Author's address:

---

Permission to make digital or hard copies of all or part of this work for personal or classroom use is granted without fee provided that copies are not made or distributed for profit or commercial advantage and that copies bear this notice and the full citation on the first page. Copyrights for components of this work owned by others than ACM must be honored. Abstracting with credit is permitted. To copy otherwise, or republish, to post on servers or to redistribute to lists, requires prior specific permission and/or a fee. Request permissions from [permissions@acm.org](mailto:permissions@acm.org).

© 2022 Association for Computing Machinery.

0730-0301/2022/9-ART \$15.00

<https://doi.org/10.1145/nnnnnnnn.nnnnnnnn>

Table 1. Statistics of those 73/100 models that we tested for the first 100 models in ABC dataset under *10k/test/2048* folder. *#s* is the number of generated medial spheres. We show the two-sided Hausdorff error  $\epsilon$  to measure the surface reconstruction accuracy using our generated medial meshes.  $\epsilon^1$  is the one-sided Hausdorff distance from the original surface to the surface reconstructed from MAT, and  $\epsilon^2$  is the error in reversed side. Models marked in blue are remeshed by removing degenerated faces as shown in Fig. 1. Models with  $\star$  use different value of thinning parameter  $\sigma = 0.1$  (default  $\sigma = 0.3$ ). We also show the Euler characteristics as “ $E$ ” (ground truth as “GT  $E$ ”) for evaluating the topology, the incorrect ones are marked in color teal.

Model	#s	$\epsilon^1$	$\epsilon^2$	GT $E$	$E$
00549	21k	1.282	1.151	-6	-5
01188	9.9k	0.698	0.336	-2	-2
01510 $\star$	7.7k	1.655	1.069	-2	-2
02000	7.4k	1.999	1.468	0	0
02124	15k	0.486	0.52	-8	-8
02596 $\star$	27k	1.363	0.955	-4	-2
02995	19k	0.85	3.927	1	14
03774	27k	0.152	0.115	-1	-1
03829	11k	0.607	0.609	0	0
04123	17k	0.78	3.799	-3	-1
05185	8k	1.263	1.065	-1	-1
05227	12k	0.442	0.338	-5	5
05302	7k	0.279	0.281	0	0
07181	5k	0.646	0.43	0	0
07446 $\star$	24k	0.817	0.621	0	0
07879	10k	0.364	0.324	-1	-1
08145	25k	0.635	0.101	1	7
08315	11k	0.713	3.351	-4	-4
08812	15k	0.728	0.563	1	1
08964	25k	0.251	0.132	-72	-37
09160	33k	0.619	1.706	-14	81
09624	6.8k	0.459	0.466	-4	-4
09796	29k	0.384	0.344	-3	-3
10170	15k	0.982	2.013	0	0
10470	9.7k	0.21	0.277	1	1
10595 $\star$	5.6k	1.606	1.904	0	0
10721 $\star$	9k	0.479	0.312	1	1
10836	3k	1.067	0.746	-1	1
11072 $\star$	26k	4.538	2.148	0	43
11299	18k	0.37	6.035	-24	-13
11368	11k	1.067	0.583	0	0
11476	9k	0.873	0.497	-2	-2
11507	16k	0.996	0.622	-5	-5
11527	12k	0.256	0.176	-6	-6
11628	31k	0.184	0.112	-18	-18
11790	17k	1.79	1.319	0	2
11800 $\star$	8k	0.28	0.253	1	1
11835	21k	1.032	2.252	0	-16
12047	5k	2.47	1.592	1	1
12182	9.6k	1.125	0.818	1	1
12254	19k	0.915	0.507	-2	-2
12261	3k	0.313	0.252	0	0
12280	8k	2.503	0.501	1	1
12547	9.9k	1.991	1.606	1	1
12618	38k	0.673	1.922	-16	-28
12621 $\star$	13k	1.19	0.788	-3	-3
12642	17k	0.596	0.471	-12	-12
12749	11k	0.764	0.865	1	1
12995	8k	0.804	0.657	-3	-3
13014	7k	0.243	0.179	1	1
13026	26k	2.203	0.698	-4	-2
13151	23k	0.519	0.495	0	0
13607 $\star$	19k	0.956	0.376	-13	-19
13624	17k	0.665	0.548	1	1
13652	23k	1.466	0.666	1	1
13952	13k	1.095	0.78	-1	-1
14326 $\star$	24k	1.373	0.84	-2	-2
14621	34k	0.819	2.812	-3	-9
14671	11k	0.455	0.435	0	0
14956 $\star$	6k	1.76	1.638	1	1
15006 $\star$	4k	2.056	1.589	1	1
15026	2k	0.164	0.127	1	1
15094	35k	1.016	1.045	-8	-4
15168	29k	1.359	1.118	-13	-13
15288	17k	0.244	2.142	0	0
15807 $\star$	11k	1.183	0.938	-1	-1
15875	8k	0.296	0.155	-1	-1
16150 $\star$	3k	0.899	1.045	1	1
16489	15k	0.719	0.657	-2	-2
17059	3k	3.333	3.09	1	1
17061(02)	12k	0.975	0.761	-6	-6
17061(15) $\star$	17k	1.933	1.468	-4	-29
17150	16k	1.231	0.797	1	1

Table 2. Statistics of 27/100 models that we filtered out. 3/27 contains open boundaries (OB), 9/27 contains self-intersections (SI) and the number of components is given as  $NC$ .

Model	OB	SI	NC
00250	-	-	2
00964	-	-	3
01174	x	x	5
02470	-	-	2
02728	x	x	5
04091	-	-	2
04381	-	-	2
04427	-	-	7
05675	-	x	4
06176	-	x	1
06750	-	-	2
07233	-	x	3
09413	-	-	3

Model	OB	SI	NC
10376	-	-	5
10972	-	-	9
11002	-	-	4
11037	-	-	2
11379	-	-	2
11379	-	-	2
11805	-	x	2
11925	-	-	2
12216	-	x	3
12733	-	-	3
13922	-	x	4
14046	x	x	2
15581	-	-	20
15820	-	-	2

## 2 EXTERNAL EDGE FEATURE PRESERVATION

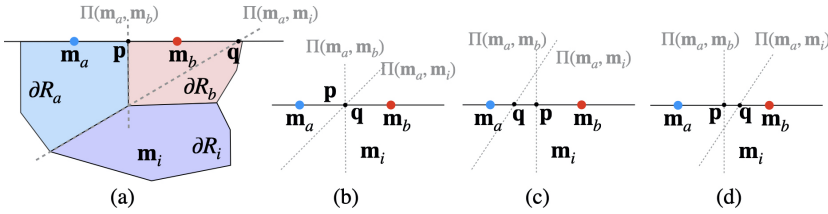


Fig. 2. (a) Illustration of RPD of three medial spheres  $m_a = (\theta_a, 0)$ ,  $m_b = (\theta_b, 0)$ , and  $m_i = (\theta_i, r_i)$ , where  $m_a$  and  $m_b$  are two neighboring zero-radius medial spheres, and  $m_i$  is a non-feature medial sphere neighboring to  $m_a$  and  $m_b$  with radius  $r_i$ . Plane  $\Pi[m_a, m_b]$  is the bisecting plane defined by  $m_a$  and  $m_b$ , and intersects the feature edge at point  $p$ . Plane  $\Pi[m_a, m_i]$  is the bisecting plane defined by spheres  $m_a$  and  $m_i$  using power distance, and intersects the feature edge at point  $q$ . (b)-(d) show three different relations between  $p$ ,  $q$ , and  $m_a$ . (b): Points  $p$  and  $q$  overlap. (c): Point  $q$  is closer to  $\theta_a$  than point  $p$  is. (d): Point  $p$  is closer to  $\theta_a$  than point  $q$  is.

One possible fix for the problem shown in Fig. 12 of the paper is to insert new feature spheres when the non-feature medial sphere whose RPC intrudes into the connection borders between two RPCs of neighboring zero-radius spheres on a sharp edge.

Suppose we have a non-feature medial sphere  $m_i = (\theta_i, r_i)$ , and two neighboring zero-radius feature spheres represented as  $m_a = (\theta_a, 0)$ ,  $m_b = (\theta_b, 0)$  respectively, as shown in Fig. 2. Note that we place zero-radius spheres  $m_a$  and  $m_b$  on the external feature edge, so the two neighboring medial spheres  $m_a$  and  $m_b$  are supposed to be connected in our final medial mesh without the interference of any non-feature medial sphere  $m_i$ . That means, the RPC of  $m_i$ , represented as  $\omega_i$ , should not intersect the feature edge  $\theta_a\theta_b$  in between  $m_a$  and  $m_b$ .

The boundary of the power cell of  $m_a$  is defined by its bounding planes  $\{\Pi[m_a, m_i] | i = 1 \dots m\}$ , where any point on the plane  $\Pi[m_a, m_i]$  is of equal power distance to these two medial spheres  $m_a$  and  $m_i$ . Note that  $\{m_i | i = 1 \dots m\}$  are the neighboring medial spheres of  $m_a$ . Apparently  $\Pi[m_a, m_b]$

is a bisector between two centers  $\theta_a$  and  $\theta_b$  since they have the same zero radius. Suppose plane  $\Pi[\mathbf{m}_a, \mathbf{m}_b]$  intersects the feature edge  $\theta_a\theta_b$  on point  $\mathbf{p} = \frac{1}{2}(\theta_a + \theta_b)$ . For any non-feature medial sphere  $\mathbf{m}_i$  that is in the vicinity of  $\mathbf{m}_a$ , the plane  $\Pi[\mathbf{m}_a, \mathbf{m}_i]$  intersects the feature edge  $\theta_a\theta_b$  on point  $\mathbf{q}$ .

We can tell whether the connection between  $\mathbf{m}_a$  and  $\mathbf{m}_b$  is invaded by  $\mathbf{m}_i$  based on the relationship between  $\mathbf{p}$ ,  $\mathbf{q}$ , and the center  $\theta_a$  on the feature edge: if point  $\mathbf{q}$  is closer to  $\theta_a$  than point  $\mathbf{p}$  (Fig. 2 (c)), then  $\mathbf{p}$  cannot be preserved in the final RPD, so the connection between  $\mathbf{m}_a$  and  $\mathbf{m}_b$  is invaded by  $\mathbf{m}_i$ . To avoid handling degeneracy, we also exclude the case when  $\mathbf{p} = \mathbf{q}$  (Fig. 2 (b)). This means  $d_{pow}(\mathbf{p}, \mathbf{m}_a) \geq d_{pow}(\mathbf{p}, \mathbf{m}_i)$ , which results in the following inequation:

$$\theta_i^\top \theta_i - (\theta_a + \theta_b)^\top \theta_i + \theta_a^\top \theta_b \leq r_i^2. \quad (1)$$

In summary, new zero-radius medial spheres should be inserted if the above Eq. (1) is satisfied for non-feature sphere  $\mathbf{m}_i$ .

### 3 ALGORITHMS

In this section we provide the detailed algorithms of (1) seam tracing as discussed in Sec. 4.3, and (2) geometry-guided thinning as discussed in Sec. 4.4.

---

#### ALGORITHM 1: Seam Tracing

---

**Data:**  $\mathcal{M}_s = \{\{\mathbf{m}_i\}, \{e_{ij}\}, \{f_{ijw}\}\}$ , the medial mesh of shape  $\mathcal{S}$

**Result:**  $E = \{e_{ij}\}$ , the edges on internal features

```

1  $Q \leftarrow \emptyset$  // queue of medial spheres on seams
2 for each vertex  $\mathbf{m}_i$  in  $\mathcal{M}_s$  of type  $T_N$  with  $N > 2$  do
3   |  $Q \leftarrow \mathbf{m}_i$ 
4 end
5 while  $Q$  not empty do
6   |  $\mathbf{m}_i \leftarrow Q.top()$ 
7   | if  $\mathbf{m}_i$  has 2 incident edges in  $E$  then
8     |   continue;
9   | end
10  | for each neighbors  $\mathbf{m}_j$  of  $\mathbf{m}_i$  do
11    |   if  $\mathbf{m}_j$  on external feature then
12      |     store edge  $e_{ij} = \{\mathbf{m}_i, \mathbf{m}_j\}$  in  $E$ 
13    |   else if all CCs of  $\mathbf{m}_i$  adjacent to CCs of  $\mathbf{m}_j$  then
14      |     store edge  $e_{ij} = \{\mathbf{m}_i, \mathbf{m}_j\}$  in  $E$ 
15    |   end
16 end

```

---

### REFERENCES

Sebastian Koch, Albert Matveev, Zhongshi Jiang, Francis Williams, Alexey Artemov, Evgeny Burnaev, Marc Alexa, Denis Zorin, and Daniele Panozzo. 2019. ABC: A Big CAD Model Dataset For Geometric Deep Learning. In *The IEEE Conference on Computer Vision and Pattern Recognition (CVPR)*.

**ALGORITHM 2:** Geometry-guided Thinning**Data:**  $\mathcal{M}_s = \{\{m_i\}, \{e_{ij}\}, \{f_{ijw}\}, \{t_{ijwk}\}\}$ , the medial mesh of shape  $\mathcal{S}$ , which contains tetrahedra  $\{f_{ijw}\}$ **Data:**  $\sigma$ , the target important factor; when reaching this, the face-edge pair  $\{f_{ijw}, e_{ij}\}$  will be not deleted**Result:**  $\overline{\mathcal{M}_s} = \{\{m_i\}, \{e_{ij}\}, \{f_{ijw}\}\}$ , the pruned medial mesh without any tetrahedron

```

1  $Q \leftarrow \emptyset$  // priority queue of  $f_{ijw}$  sorted by importance factor  $\alpha_{ijw}$ 
2 for each face  $f_{ijw}$  in non-deleted tet  $t_{ijwk}$  do
3   | compute the importance factor  $\alpha_{ijw}$ ;
4   |  $Q \leftarrow f_{ijw}$  with  $\alpha_{ijw}$ 
5 end
   /* Prune tet-face simple pairs */
6 while number of non-deleted  $t_{ijwk} \neq 0$  do
7   | for each  $f_{ijw}$  in  $Q$  do
8     | if  $f_{ijw}$  is not delete and  $f_{ijw}$  is adjacent to only 1 tet  $t_{ijwk}$  then
9       | | prune tet-face pair  $\{t_{ijwk}, f_{ijw}\}$ ;
10      | | break;
11      | end
12    | end
13 end
   /* Prune face-edge simple pairs */
14  $n_f \leftarrow 0$  // number of faces on tets that have been processed
15 while  $n_f \neq Q.size()$  do
16   |  $n_f \leftarrow 0$ 
17   | for each  $f_{ijw}$  in  $Q$  do
18     | if  $f_{ijw}$  is deleted or  $\alpha_{ijw} \geq \sigma$  then
19       | |  $n_f ++$ ;
20       | | continue;
21     | end
22     | for each  $e_{ij}$  in  $f_{ijw}$  do
23       | | if  $e_{ij}$  is adjacent to only 1 face  $f_{ijw}$  and not on external features then
24         | | | prune face-edge pair  $\{f_{ijw}, e_{ij}\}$ ;
25         | | | break;
26       | | end
27     | end
28     | if  $f_{ijw}$  is deleted then
29       | | break;
30     | end
31     |  $n_f ++$ ;
32   | end
33 end

```